An Isothermal Temperature Source with a Large Surface Area using the Metal-Etched Microwick-Inserted Vapor Chamber Heat Spreader

Jeung Sang Go*, Kyung Chun Kim
School of Mechanical Engineering, Pusan National University, 30 Jangjeon-dong, Geumjeong-gu, Busan 609-735, Korea

For use of the thermal cycle of the biochemical fluid sample, the isothermal temperature source with a large surface area was designed, fabricated and its thermal characterization was experimentally evaluated. The comprehensive overview of the technology trend on the temperature control devices was detailed. The large surface area isothermal temperature source was realized by using the vapor chamber heat spreader. The cost-effectiveness and simple manufacturing process were achieved by using the metal-etched wick structure. The temperature distribution was quantitatively investigated by using IR temperature imaging system at equivalent temperatures to the PCR thermal cycle. The standard deviation was measured to be within 0.7℃ for each temperature cycle. This concludes that the presented isothermal temperature source enables no temperature gradient inside bio-sample fluid. Furthormore it can be applied to the cooling of the electronic devices due to its slimness and low thermal spreading resistance.

Key Words : Isothermal Temperature, Vapor Chamber, Heat Spreader, Metal-Etched Wick

Nomenclature

A_f : Heated surface area of sample fluid
L_c : Characteristic length
V_f : Volume of sample fluid
R : Thermal resistance
c_p : Heat capacity of sample fluid
h : Convection heat transfer coefficient
k_f : Thermal conductivity of sample fluid
t_f : Thickness of sample fluid
ΔP_{capil} : Capillary pressure
ΔP_f : Liquid pressure drop
ΔP_v : Vapor pressure drop
ρ_f : Density of sample fluid
τ_t : Thermal time constant
τ_s : Settling time constant

* Corresponding Author,
E-mail : micros@pusan.ac.kr
TEL : +81-52-510-3512; **FAX** : +81-52-512-5236
School of Mechanical Engineering, Pusan National University, 30 Jangjeon-dong, Geumjeong-gu, Busan 609-735, Korea. (Manuscript **Received** May 19, 2003; **Revised** February 6, 2004)

1. Introduction

With the advent of the biotechnology era, the temperature control device has been spotlighted. The precise thermal cycle device has become an essential part of the polymerase chain reaction (PCR) for gene diagnosis, (Mullis et al., 1994) and also of a micro chemical plant for chemical reaction (Ehrfeld et al., 2000). The technology tree on thermal cycle device can be categorized and evaluated in viewpoint of the thermal management rather than control time and power consumption.

One view point is the thermal time constant. For surrounding disturbance with regard to heating and cooling, the biochemical fluid experiences the transient heat transfer in its thermal environment until the temperature reaches at the steady state. Generally, the shorter thermal time constant leads to the faster response. Figure 1 shows the schematic transient and steady state

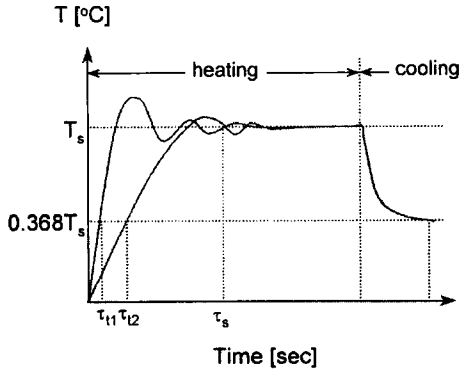

Fig. 1 Transient and steady state temperature response

temperature responses of sample fluid with different thermal time constant. To describe the transient heat transfer, the Lumped capacitance method can be used. The temperature response of sample fluid with respect to time can be obtained from energy balance (Incropera and Dewitt, 1996).

$$\tau_t=\frac{1}{hA_f}(\rho_f V_f c_p)=\rho_f c_p\frac{1}{h}\left(\frac{V_f}{A_f}\right)=\rho_f c_p\frac{t_f}{h} \quad (1)$$

where ρ_f, c_p, t_f and h denote the density, heat capacity, thickness of sample fluid and convection heat transfer coefficient, respectively. V_f and A_f are the volume and the surface area of sample fluid.

Since the density and the heat capacity are directly specified as sample fluid is decided, fast response can be obtained by decreasing film thickness and increasing the convection heat transfer coefficient. The miniaturized and micromachined chamber PCR devices use thin film to obtain fast temperature cycle (Waters et al., 1998 ; Ross et al., 1998). Compared with fairly larger conventional PCR systems, film thickness can be decreased to hundred microns so that the PCR time can be proportionally reduced. The microchannel heat exchanger uses a high heat transfer coefficient (Tuckerman and Pease, 1981). The heat transfer coefficient is inversely proportional to the hydraulic diameter. The microchannel flow-through PCR devices were fabricated to increase yield rate (Kopp et al., 1998 ; Schneegaß et al., 2001 ; Burns et al., 1998).

Modeling of the Lumped capacitance can be verified by considering the Biot number, which is a measure of the temperature drop in sample fluid.

$$Bi=\frac{hL_c}{k_f} \quad (2)$$

where L_c denotes the characteristic length of the sample fluid and k_f denotes the thermal conductivity of the sample fluid. For the condition of $Bi \ll 0.1$, a uniform temperature distribution across the sample fluid can be assumed reasonably. In the micromachined devices, the characteristic length is equal to film thickness. As a result, the Biot number is less than 0.1, indicating that the Lumped capacitance method is available.

The second viewpoint is the thermal resistance. For the steady state heat transfer, thermal resistance is a major characteristic of a thermal system. Based on the Fourier's law of cooling, the thermal resistace of sample fluid is expressed as :

$$R=\frac{t_f}{k_f A_f} \quad (3)$$

However, the aforementioned micromachined devices face large thermal resistance due to their small surface area in spite of their thin film thickness of sample fluid. Therefore, the serious temperature difference within sample fluid is encountered. To this end, the larger heat conduction surface area enables the micromachined devices to have uniform temperature and faster temperature response simultaneously. However, there is a difficulty in obtaining an entire isothermal temperature surface on a large surface area. A heater and sensor array should be installed for uniform heating of large surface area and the feedback control of temperature and observation of heat spots induced by local heating.

In this paper, a high performance isothermal temperature source on large surface area using vapor chamber heat spreader is attempted for the application of the thermal treatment of the DNA and cell. Analytically, its working principle and design consideration under the hydrodynamic constraint are detailed. Moreover the cost-effective metal microwick-inserted temperature source is presented. Finally, the quantitative thermal

characterization of the temperature source are performed at the equivalent temperatures of the PCR cycle.

2. Working Principle and Design

The vapor chamber heat spreader has been developed intensively for the future cooling solution of a high performance computer system due to its low spreading thermal resistance (Take and Webb, 1999 ; Mehl et al., 2000). It is a closed vacuum device containing the wick structure which drives capillary pressure to circulate working fluid inside chamber. The heat is transferred by the phase change of working fluid, repeating evaporation and condensation continuously. Especially, the uniform temperature on upper surface can be obtained by saturation temperature of working fluid.

The vapor chamber heat spreader is commonly composed of microchannels for capillary driven flow and vapor flow channel (Fig. 2). For stable run, the capillary pressure, ΔP_{capil}, induced by the microwick must exceed summation of pressure drops such as the liquid pressure drop, ΔP_f, vapor pressure drop, ΔP_v and so on. Based on the heat pipe theory (Faghri, 1995), the hydrodynamic condition is interpreted as follows:

$$\Delta P_{capil} \geq \Delta P_f + \Delta P_v + \sum \Delta P_{etc} \quad (4)$$

The wick structure decides thermal capacity of the vapor chamber heat spreader. In stead of using conventional wick structures such as mesh screen wick or sintered porous metal, the metal-etched microwick for simple assembly and cost-effective manufacturing was proposed. Figure 3 shows a SEM photograph of the metal-etched wick plate of 40 mm×40 mm. Since the metal plate was etched isotropically from both sides, the minimum channel width possible to fabricate was confined by its thickness. The minimum width for the 110 μm-thick metal plate was obtained to be 150 μm thick for liquid phase flow and the 100 μm-wide wall spacing was considered.

The comprehensive simulation was carried out to evaluate the hydraulic constraint under the heat input of 20 W in which the sufficient

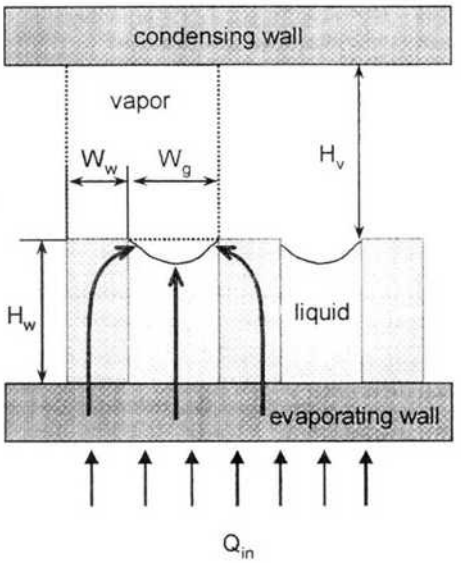

Fig. 2 Cross-sectional view of vapor chamber heat spreader

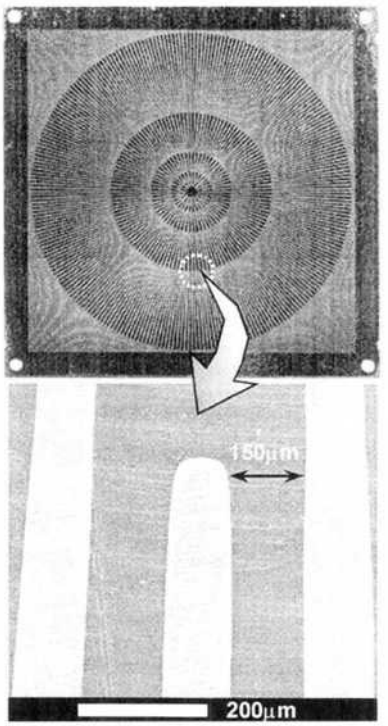

Fig. 3 SEM photos of the metal-etched wick structure

heat was obtained for the PCR temperatures based on the Newton's law of cooling. The capillary pressure for one wick structure was calculated to be 278.2 Pa. The vapor pressure drop and the liquid pressure drop were 211 Pa and 4.5 Pa, respectively. Therefore, the residual capillary pressure of 62.7 Pa can provide enough pumping pressure to drive working fluid.

3. Fabrication and Assembly

Figure 4 shows the schematic view of the vapor chamber heat source. Fabrication process of the vapor chamber heat spreader starts with making the vapor chamber housing. The metal-etched wick structure is just inserted into the vapor chamber. Then, the vapor chamber housing is permanently sealed with metallic welding to maintain vacuum state. The copper tube for feed-through of working fluid is fixed to the vapor chamber and also welded.

The wick structure was made of stainless steel and the vapor chamber was made of aluminum. The acetone was used as working fluid, which has no chemical reaction to both materials. The fabricated vapor chamber heat spreader was a rectangular flat plate with size of 83 mm × 69 mm and the thickness of the vapor chamber was 1.67 mm. Its total volume was measured to be 6 ml. The optimum amount of working fluid was charged and was frozen in liquid nitrogen. To remove non-condensable gases, the vapor chamber was evacuated at the level of vacuum state of about 10^{-3} torr and then the copper feed-through tube was mechanically sealed.

In this experiment, the acetone working fluid was charged to 30% of the total vapor chamber volume. By varying the charging ratio of working fluid, the heater temperature at the heat input of 20 W was examined. The minimum heater temperature was obtained at the charging ratio of 30 %. When working fluid was charged less than 30 %, the dry-out appearred resulting in the occurrence of unstable operation. When the charging ratio was greater than 30%, the operation was still stable, but the heater temperature increased due to thick film thickness of the working fluid in the microwick.

4. Experimental Setup

Figure 5 illustrates the test apparatus for thermal performance measurement of the isothermal temperature source. Electrical power was applied to the ceramic heater using a DC power supply (HP, E3620A). The size of the ceramic heater was 10 mm × 10 mm. The power meter (YOKOGAWA, WT200) measured precise power consumption transferred to the vapor chamber heat spreader. Three J-type thermocouples (OMEGA,

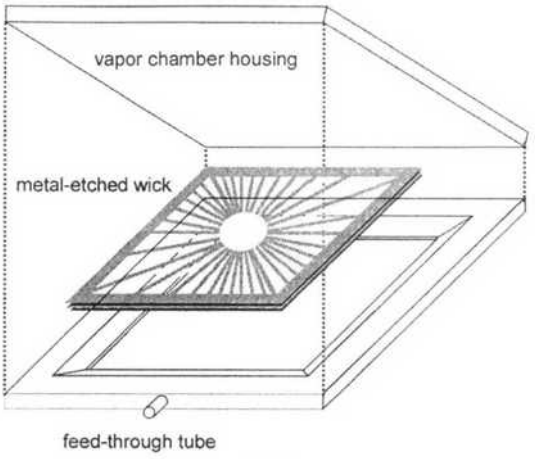

Fig. 4 Configuration of the vapor chamber heat spreader

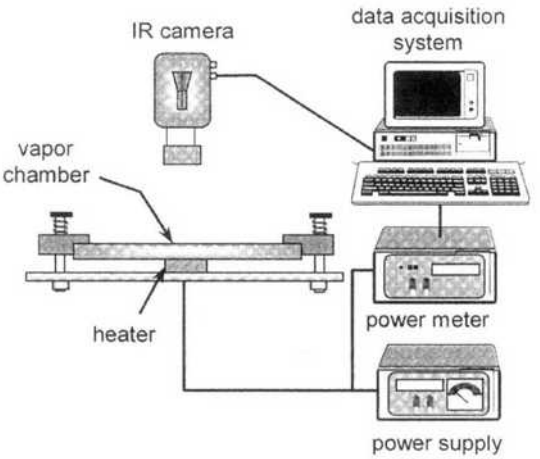

Fig. 5 Schematic diagram of instrumentation for the thermal measurement

CHAL-010) were instrumented to evaluate the performance of the isothermal temperature source. The temperature of the ceramic heater was measured to monitor the sudden increase in the temperature resulting from the dry-out. In addition, the upper surface temperature and the ambient temperature were measured to quantify the performance of the isothermal temperature source. The thermal interface material (Thermax, HF-60110BT) with a high thermal conductivity of 0.05 W/m-K was inserted between the vapor chamber and the ceramic heater to minimize the thermal contact resistance. A data acquisition system (HP, 34970A) recorded temperature data. An IR imaging system (ThermaCam Inframetrics, SC 1000) investigated the temperature distribution on the upper surface of the vapor chamber heat spreader.

5. Results and Discussion

At the equivalent temperature of the PCR thermal cycle, the thermal uniformity of the vapor chamber heat spreader were examined. The PCR thermocycler repeats three steps of temperature cycle with denaturation of 95℃, annealing of 55℃ and extension of 72℃. To obtain such temperatures, the applied power was tuned to 18.42 W, 6.76 W and 11.72 W, respectively. The vapor chamber was cooled by the natural convection heat transfer. Fig. 6 visualizes temperature distribution on the upper surface of the vapor chamber heat spreader. Even though the surface area of the vapor chamber heat spreader was dominantly large compared to the heater size, temperature distribution was negligible. For the quantitative characterization, the temperature measurement was carried out along the vertical and horizontal line at the center. As shown in Fig. 7, high performance isothermal temperature source for each temperature was obtained. The standard deviation was measured to be within 0.7℃. Furthermore, it was determined that there was no temperature gradient resulting from the film condensation on the large surface area. Therefore, the temperature of the isothermal heat source can be obtained by the saturation temperature of working fluid.

Secondly, the transient response of the temperature source was examined by varying the applied

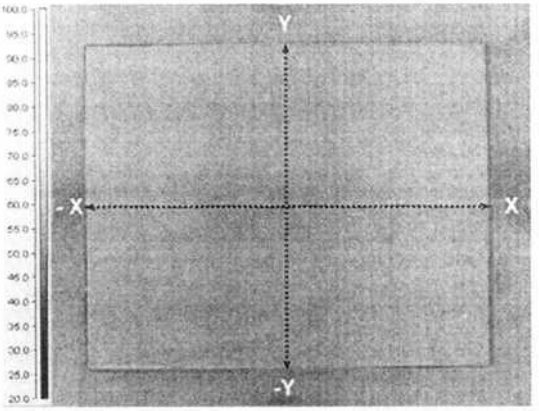

(a) For 55℃ with heat input of 6.76 W

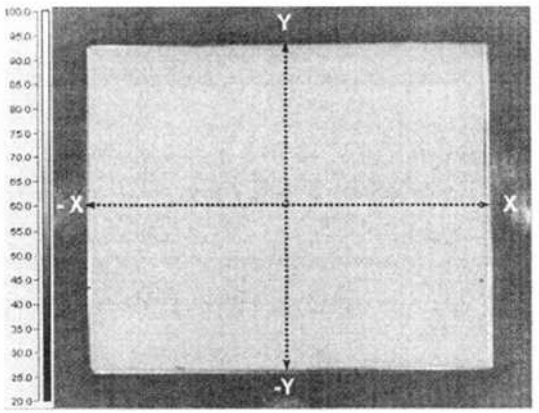

(b) For 72℃ with heat input of 11.72 W

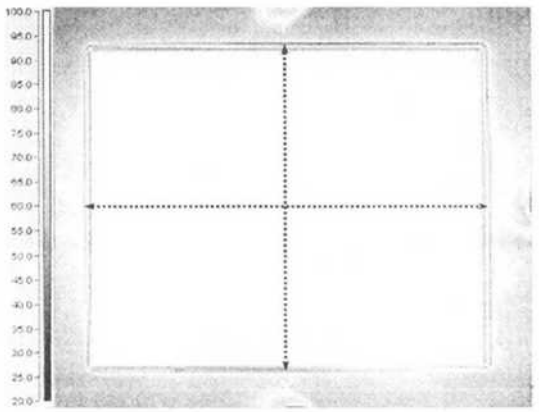

(c) For 95℃ with heat input of 18.42 W

Fig. 6 Comparative graphical temperature distribution

heat input. The temperature was measured by the thermocouple installed on the upper surface. This measurement is valid since there is no significant temperature variation on the upper surface area. As shown in Fig. 8, the temperature was kept constant after the steady state was reached. However long settling time was shown since the natural convection heat transfer was used in this experiment. This can be solved by using forced convection cooling.

To investigate effect of the forced convection, the vapor chamber heat source was compared to the plain aluminum plate with the same size by measuring surface temperature distribution. Fig. 9 shows comparative temperature distribution under the natural convection cooling and the air impinging cooling of 3 m/s, respectively. In case of the vapor chamber heat source, temperature distribution was always kept small for both cases. This result also implies that the

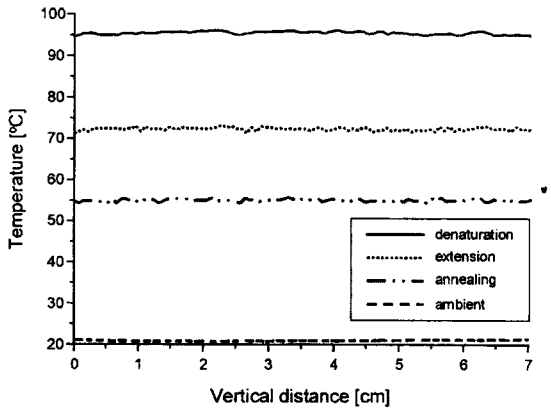

(a) Along a horizontal line

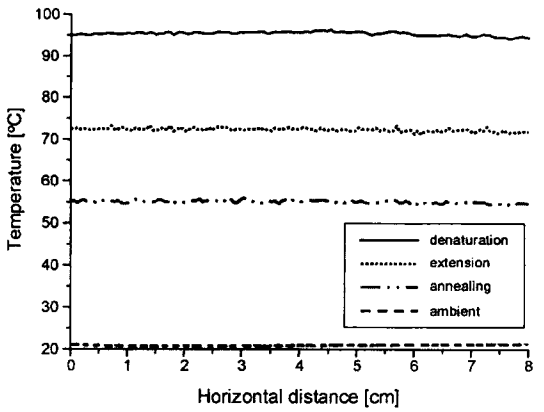

(b) Along a vertical line

Fig. 7 Temperature measurement on the isothermal temperature source

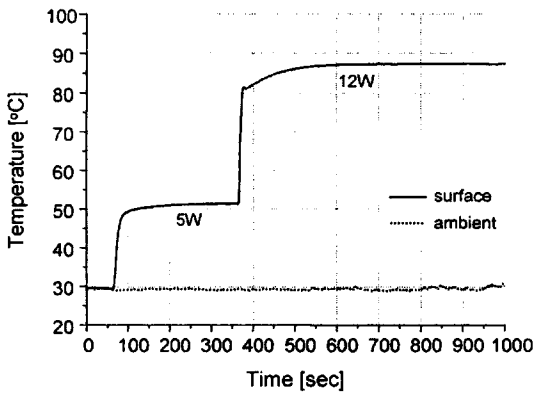

Fig. 8 Transient temperature response by varying heat inputs

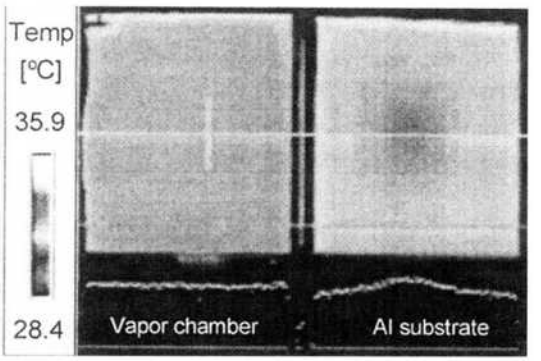

(a) For the natural convection heat transfer

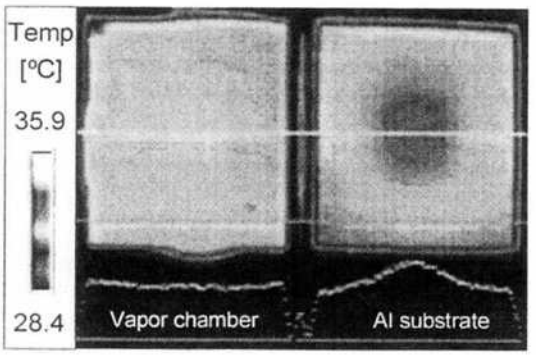

(b) For the forced convection heat transfer with air blowing of 3 m/s

Fig. 9 Comparative temperature distribution in the isothermal heat source and in the plain aluminum plate

vapor chamber temperature source is very resistant to the external thermal disturbance. On the other hand, the temperature distribution of the plain aluminum plate was changed significantly at air cooling. This indicates that when conventional heater array are used for temperature source, the heater array must be controlled independently with feedback control from temperature sensing.

6. Conclusions

The vapor chamber heat spreader containing the metal-etched microwick structure has been proven to be applicable as an isothermal temperature source with large surface area to reduce the spreading thermal resistance for the application of the biochemical temperature treatment device.

Theoretically, to ensure its proper working, the hydrodynamic constraint based on relationship between the capillary pressure resulting from the metal-etched microchannel and total pressure drop was considered. For the experimental evaluation, the low cost metal-etched microwick structure was fabricated and was inserted to the vapor chamber heat spreader. It was determined that the fabricated vapor chamber heat spreader showed very little temperature drop on the large surface area for the various heat inputs. Moreover, its temperature distribution was very resistant to the external disturbance. In addition, it was newly found that the temperature drop on the upper surface induced by film condensation was negligible.

For further research, the cyclic temperature response of the isothermal temperature source must be characterized for the biochemical application. In addition, it is challenging to apply it to cooling of slim mobile systems such as notebook computers and PDA, when considering the thickness of the fabricated vapor chamber heat spreader.

Acknowledgment

The authors would like to thank all members of Microcooling team in Samsung Advanced Institute of Technology (SAIT) for the technical support. Especially, the authors appreciate T. G. Kim to help fabrication of the vapor chamber heat spreader. In addition, this work has been partially supported by National Research Laboratory Program in Korea.

References

Burns, M. A., Johnson, B. N., Brahmasandra, S. N., Handique, K., Webster, J. R., Krishnan, M., Sammarco, T. S., Man, P. M., Jones, D., Heldsinger, D., Mastrangelo, C. H. and Burke, D. T., 1998, "An Integrated Nanoliter DNA Analysis Device," *Science*, Vol. 282, pp. 484~487.

Ehrfeld, W., Hessel, V. and Löwe, H., 2000, *Microreactors*, Wiley-VCH, Verlag GmbH, Weinheim.

Faghri, A., 1995, *Heat Pipe Science and Technology*, Taylor and Francis Ltd.

Incropera, F. P. and Dewitt, D. P., 1996, *Fundamentals of Heat and Mass Transfer*, John Wiley & Sons.

Kopp, M. U., de Mello, A. J. and Manz, A., 1998, "A Chemical Amplification : Continuous-Flow PCR on a Chip," *Science*, Vol. 280, pp. 1046~1047.

Mehl, D., Dussinger, P. and Grubb, K., 2000, "Use of Vapor Chambers for Thermal Management," *Thermacore Inc.*.

Mullis, K. B., Ferre F. and Gibbs, R. A., 1994, *The Polymerase Chain Reaction*, Birkhauser, Boston.

Ross, P. L., Davis, P. A. and Belgrader, P., 1998, "Analysis of DNA Fragments from Conventional and Microfabricated PCR Devices Using Delayed Extraction MALDI-TOF Mass Spectrometry," *Anal. Chem.*, Vol. 70, No. 10, pp. 2067~2073.

Schneegaß, I., Brautigam, R. and Kohler, J. M., 2001, "Miniaturized Flow-through PCR with Different Template Types in a Silicon Chip Thermocycler," *Lab on a chip*, pp. 42~49.

Take, K. and Webb, R. L. 1999, "Thermal Performance of Integrated Plate Heat Pipe with a Heat Spreader," *Advances in electronic packa-*

ging, Vol. 2, pp. 2113~2120.

Tuckerman, D. B. and Pease, R. F. W., 1981, "High-Performance Heat Sinking for VLSI," *IEEE Electron Device Letters*, Vol. EDL-2, No. 5, pp. 126~213.

Waters, L. C., Jacobson, S. C., Kroutchinina, N., Khandurina, J., Foote, R. S. and Ramsey, J. M., 1998, "Microchip Device for Cell Lysis, Multiplex PCR Amplification and Electrophoretic Sizing," *Anal. Chem.*, Vol. 70, No. 1, pp. 158~159.